Protein folding under confinement: A role for solvent

Del Lucent*, V. Vishal†, and Vijay S. Pande*†‡§

*Biophysics Program and Departments of †Chemistry and ‡Structural Biology, Stanford University, Stanford, CA 94305

Edited by Stephen L. Mayo, California Institute of Technology, Pasadena, CA, and approved May 8, 2007 (received for review September 20, 2006)

Although most experimental and theoretical studies of protein folding involve proteins *in vitro*, the effects of spatial confinement may complicate protein folding *in vivo*. In this study, we examine the folding dynamics of villin (a small fast folding protein) with explicit solvent confined to an inert nanopore. We have calculated the probability of folding before unfolding (P_{fold}) under various confinement regimes. Using P_{fold} correlation techniques, we observed two competing effects. Confining protein alone promotes folding by destabilizing the unfolded state. In contrast, confining both protein and solvent gives rise to a solvent-mediated effect that destabilizes the native state. When both protein and solvent are confined we see unfolding to a compact unfolded state different from the unfolded state seen in bulk. Thus, we demonstrate that the confinement of solvent has a significant impact on protein kinetics and thermodynamics. We conclude with a discussion of the implications of these results for folding in confined environments such as the chaperonin cavity *in vivo*.

chaperonin mechanism | explicit solvent | distributed computing | molecular dynamics

How proteins fold into a unique native structure is an important unanswered question. There have been a number of experiments and computer simulations that have provided insight into the mechanism by which folding occurs (1, 2). Most of these experiments and simulations measure the dynamics of proteins in infinite dilution. However, bulk solvent is different from the cellular environment in which proteins truly fold. *In vivo*, protein dynamics occur in the context of the crowded cellular milieu and in confined spaces such as the chaperonin cavity, the proteosome, the ribosome exit tunnel, the translocon, etc. When considering these factors it is reasonable to assume that proteins may experience different energy landscapes when folding *in vivo* than in bulk, and these differences may constitute a significant piece of the folding puzzle.

Confinement has been previously treated both analytically and via simulation using polymer physics models (3–10). These models predict that by excluding more extended structures confinement reduces the conformational entropy of the unfolded-state ensemble. This restriction leads to the relative stabilization of the folded state. These models are in qualitative accord with recent experiments that have shown accelerated folding of small proteins in chaperonin mutants possessing decreased cavity volume (11). Despite the elegance and intuitiveness of these models, they omit details that may be important when thinking of folding *in vivo*.

For example, it is known that solvent plays a critical role in protein folding, as most of the free energy for folding comes from maximizing solvent entropy (because of the molecular nature of hydrophobicity). Polymer models for confined folding do not consider the effect of confinement on the solvent and its subsequent effects on protein stability. Although explicit solvent complicates analytical models and makes simulation more computationally demanding, including explicit solvent allows one to account for solvent-mediated effects in folding mechanism. For example, it has been shown for simulations of small proteins that implicit and explicit solvent models can yield similar folding rates but different folding mechanisms (12, 13). Because "confinement" includes confined solvent and confined protein and nanoscopic water has been shown (by experiment and simulation) to behave differently from bulk water both thermodynamically and kinetically (14–16), we expect that treating water explicitly is crucial to properly describing the dynamics of protein folding in confined spaces.

Recent folding simulations of purely polymeric models and models that treat solvent explicitly have shown drastically different results. Specifically, Ziv *et al.* (10) have suggested that for a small helical peptide helix formation is stabilized upon confinement to a cylindrical cavity. These results were explained in terms of polymer entropy arguments as described above. On the other hand, Sorin and Pande (17) have recently shown that for an α-helical peptide confined to a single-walled carbon nanotube with explicit solvent the opposite effect was observed; the unfolded state is stabilized and the helix unfolds. This observation was explained in terms of solvent entropy. In bulk, protein folding maximizes solvent entropy, but in a confined system solvent entropy is already limited and protein–protein interactions experience a reduced entropic stabilization relative to protein–water interactions.

These results motivate a direct comparison of protein folding in the context of both polymer confinement and solvent confinement. It is also important to study these effects in systems with more complicated protein topologies (wherein secondary structure formation is not the sole determinant of the native state). Here, we study the folding of a small protein [the villin headpiece; Protein Data Base ID code 1VII (18)] confined to an inert nanopore (a repulsive sphere with a radius of 28 Å) using atomistic molecular dynamics and the TIP3P explicit solvent model (19). The villin headpiece is a 4.2-kDa, fast-folding protein (20) that consists of three helices surrounding a hydrophobic core of three phenylalanine residues (Fig. 1*D*).

To probe the effects of confinement on the protein versus the solvent, we constructed several different versions of the nanopore. In one set of simulations, the solvent can pass freely through the confining boundary while the protein remains confined (Fig. 1*B*). In another set of simulations, both the protein and the solvent are confined (Fig. 1*C*). A third set of simulations with no confinement was performed as a control (Fig. 1*A*). Using this set of models, we are able to directly compare the effects of protein-only confinement to protein and solvent confinement without changing solvation models. Using these simulations, we are able to observe a folding effect arising from polymeric confinement and an unfolding effect arising from solvent confinement. These two effects are mechanistically different from each other. In particular, the system wherein both protein and solvent are confined shows unfolding to a different unfolded state than that seen in bulk.

Author contributions: V.V. and V.S.P. designed research; D.L. and V.V. performed research; D.L. analyzed data; and D.L. wrote the paper.

The authors declare no conflict of interest.

This article is a PNAS Direct Submission.

Abbreviation: $dRMSD_{C\alpha}$, distance rmsd of the protein α carbons from their native positions.

§To whom correspondence should be addressed. E-mail: pande@stanford.edu.

This article contains supporting information online at www.pnas.org/cgi/content/full/0608256104/DC1.

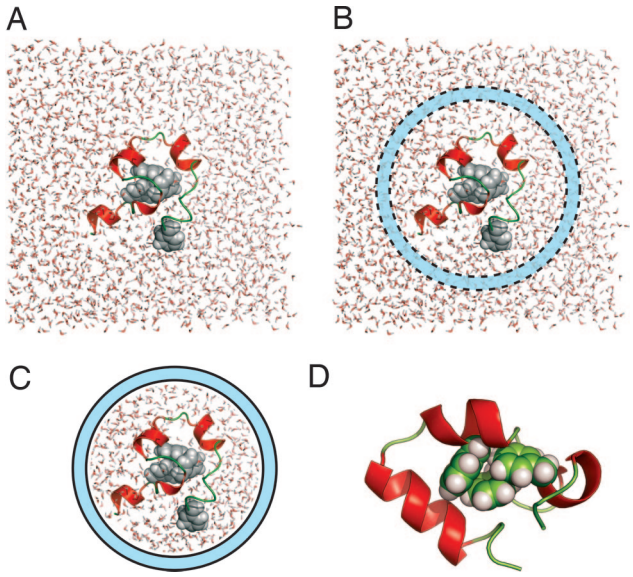

Fig. 1. The setup for our confinement simulations. (*A*) Folding of the villin headpiece was simulated in bulk, as well as in confinement (via an inert nanopore with a radius of 28 Å). (*B*) For one set of simulations the confining potential was constructed such that villin was confined but the surrounding solvent was able to pass freely through the barrier. (*C*) For another set of simulations, the confining potential was constructed such that both villin and the solvent were confined. (*D*) Villin is a small 36-residue protein with three α-helices and a hydrophobic core consisting of three phenylalanine residues.

Results and Discussion

The P_{fold} method was used to assess the effect of confinement on folding kinetics and thermodynamics (see *Methods* for an explanation of P_{fold}). We can determine the effect of confinement on folding by correlating the P_{fold} values of our confined (perturbed) and unconfined (unperturbed) systems. These correlations allow us to compare two systems and determine which is more likely to fold (Fig. 2*A*). We can also infer changes in native-state stability ($\Delta\Delta G_{\text{F}}$; Fig. 2*A*) and changes in mechanism such as a shift or broadening of the transition state (Δx_{TS}, $\Delta\sigma$; Table 1).

When we correlate the P_{fold} of the bulk-like system (Fig. 1*A*) with the protein-only confinement system (Fig. 1*B*), we find that P_{fold} increases upon confinement (Fig. 2*B*). Therefore, confining the protein increases the probability of folding before unfolding. From our estimate of $\Delta\Delta G_{\text{F}}$ (Table 1) we can see that the native state is stabilized ($-1.01 \pm 0.19\, k_{\text{B}}T$). Using the method of Zhou and Dill (3), one would predict analytically that a system of this size would be stabilized by $-0.35\, k_{\text{B}}T$. As a positive control, these simulations were repeated at larger confining radii. The estimated $\Delta\Delta G_{\text{F}}$ agrees very well with the values predicted from analytical methods. Thus our simulations agree qualitatively with predictions from polymer theory [see supporting information (SI) *Text* for details concerning the analytical calculation of $\Delta\Delta G_{\text{F}}$ for this system].

We can also see from our estimation of barrier width ($\Delta\sigma$; Table 1) and transition-state shift (Δx_{TS}, Table 1) that polymeric confinement is mechanistically different from bulk folding. By the Hammond postulate, these data also support a highly destabilized unfolded state. Thus, we observe that protein-only confinement increases folding by destabilizing the unfolded state, which is consistent with predictions based purely on polymer entropy.

However, when protein and solvent were both confined (Fig. 1*C*), the probability of folding before unfolding decreased (Fig. 2*C*). Our estimate of native-state stability shows that the folded state is destabilized under these conditions ($\Delta\Delta G_{\text{F}} = 1.05\, k_{\text{B}}T$; Table 1). We also observed that the transition state is shifted toward the folded state and the barrier does not broaden (Table 1). This finding implies a different mechanism from bulk folding and folding with only protein confined. Also, in terms of the Hammond postulate, these data agree with our prediction of decreased native-state stability. Overall, these observations imply that confined solvent has a negative effect on protein folding.

The errors reported in Table 1 arise from the statistical uncertainty in our P_{fold} correlations. Although there is some spread in the data, it still remains that the correlations are significantly nonlinear (which is further demonstrated by Fig. 2*D*, which directly compares protein-only confinement to protein and solvent confinement). The scatter in the data implies that while the values reported in Table 1 may not be sufficiently precise to be truly quantitatively useful these data can still yield a reasonable qualitative and potentially semiquantitative assessment of kinetic and thermodynamic perturbations to folding resulting from confinement. Despite this scatter it should be noted that the estimates of native-state stability are self-consistent in that the $\Delta\Delta G_{\text{F}}$ from Fig. 2*D* is approximately equal to the difference of the $\Delta\Delta G_{\text{F}}$ from Fig. 2 *B* and *C*.

Together, our results indicate that there is a polymeric confinement effect (Fig. 2*B*) in which the native state is stabilized and a solvent-confinement effect (Fig. 2*C*) in which the unfolded state is stabilized. It is important to note that the system depicted in Fig. 1*C* confines both protein and solvent. Thus it must also intrinsically contain any polymeric-confinement effects observed in the system shown by Fig. 1*B*. This finding implies that the solvent-confinement effect is greater in magnitude than the polymer-confinement effect for our system. It is also consistent with Zhou and Dill's model (3) in that large (5–10 $k_{\text{B}}T$) stabilizations occur only for larger systems that are extremely confined (such that the confining volume is only slightly larger than the volume of the native state).

When considering how these effects arise, it is convenient to look at a distribution of states according to various metrics. Fig. 3 shows the 2D histogram of distance rmsd of the protein α carbons from their native positions ($\text{dRMSD}_{\text{C}\alpha}$) and helicity (as these plots were constructed from nonequilibrium data, contours should not be taken to imply free energy, rather these plots are included to show the different regions of conformation space explored under confinement). We can see that in the bulk-like system, there are a number of states with high $\text{dRMSD}_{\text{C}\alpha}$ (>7 Å) and moderate amounts of secondary structure (helicity) (Fig. 3*A*). This result is consistent with experimental observations of unfolded villin (21). These unfolded states have greatly reduced population in the polymeric confinement system (Fig. 3*B*), which is in agreement with the P_{fold} correlation shown in Fig. 2*B*. The system with protein and solvent confined is also missing this population of states but contains a new population with low $\text{dRMSD}_{\text{C}\alpha}$ and low helicity (Fig. 3*C*). The same trend is observed in Fig. 3 *D–F* with radius of gyration. Thus in the absence of confinement, the unfolded state is populated mostly by more expanded structures ($R_{\text{g}} \approx 60\%$ of what would be expected from an ideal polymer chain of the same length) that contain moderate amounts of secondary structure. In contrast, with protein and solvent confined the unfolded state is populated by compact structures with very little secondary structure. Direct observation of trajectories from these simulations has revealed that this compact unfolded state occurs when the protein migrates to the interface between the solvent and the confining wall. This loss of secondary structure is consistent with observations from Sorin and Pande (17) in which molecular dynamics simulations of an α-helix confined to a single-walled carbon nanotube with explicit solvent showed unfolding. Sorin and Pande's argument states that this loss of secondary structure results from the reduced entropy of confined solvent, which is completely consistent with our observations, as the free-energy difference between a

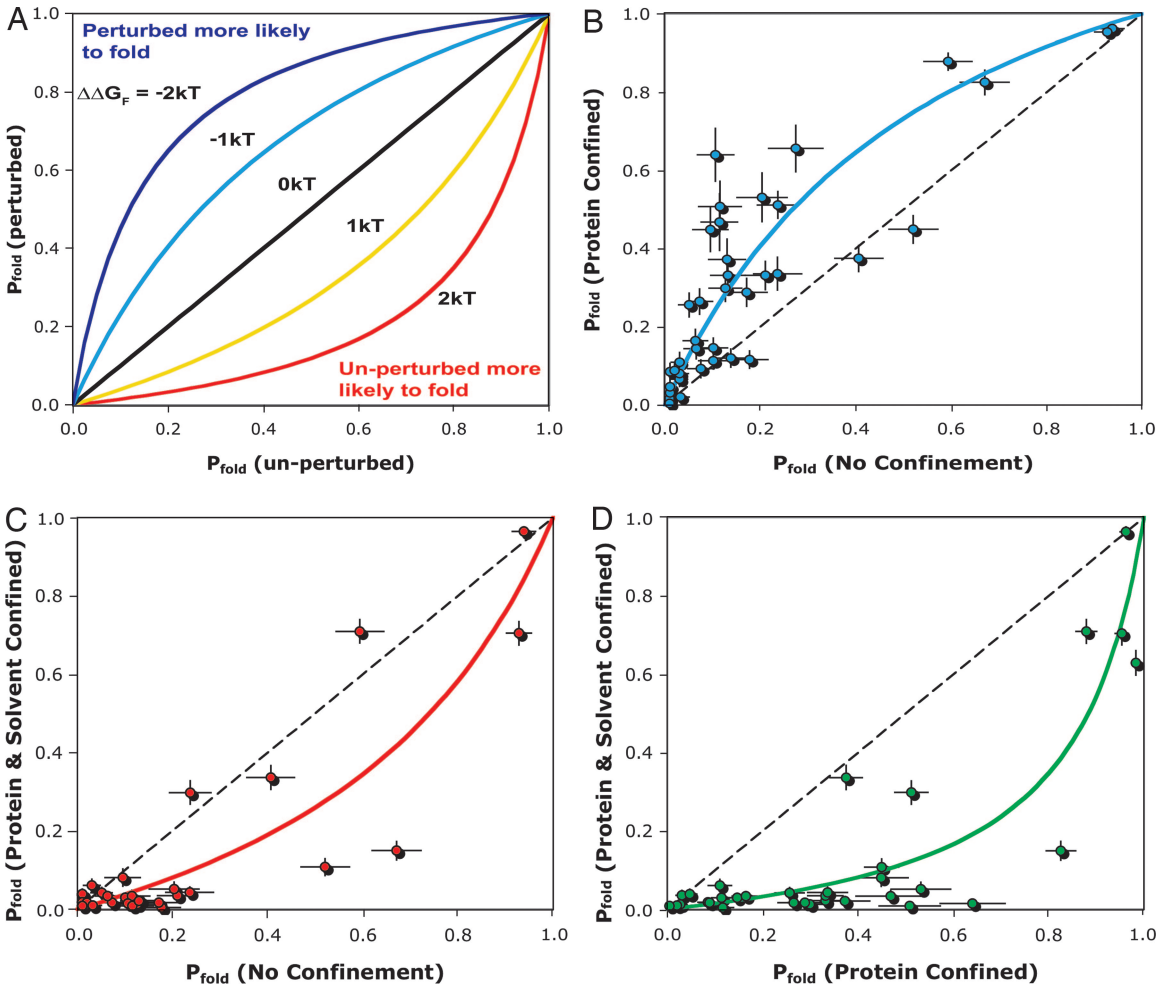

Fig. 2. The probability of folding before unfolding (P_{fold}) was computed for a number of villin conformations under conditions of no confinement, confinement of only protein, and confinement of both protein and solvent. (*A*) Illustration of how correlations in P_{fold} correspond to differences in native-state stability ($\Delta\Delta G_F$). (*B*) The P_{fold} correlation between the unconfined system and the system with only protein confined. (*C*) The correlation between the unconfined system and the system with both protein and solvent confined. (*D*) The correlation between the system with protein and solvent confined and the system with only protein confined. Error bars represent the error about the mean of a Bernoulli distribution. The trend lines are fits of the data to the function $y = x/x + e^{\beta\Delta\Delta GF}(1 - x)$, where β is temperature $\times$ Boltzmann's constant and the values for $\Delta\Delta G_F$ are those shown in Table 1 (see ref. 34 and *SI Text* for a derivation for this analytical function for P_{fold} correlation).

protein–protein hydrogen bond and a protein–water hydrogen bond would be decreased at the solvent interface. These results seem to support a collapsed globule type mechanism (22) when protein and solvent are confined.

Conclusions

We have observed both a "folding effect" arising from polymeric confinement and an "unfolding effect" arising from solvent confinement. The folding effect we observe is qualitatively consistent with the polymer entropy model proposed by Zhou and Dill (3). The observed agreement with previous simpler models and analytic theory serves as an excellent validation for our simulation methodology. Likewise, the fact that we observe an unfolding effect when water is treated explicitly implies that polymer entropy models alone may be insufficient to describe confined folding for all systems. In addition, because our confining potential is completely repulsive, we can conclude that this unfolding action does not arise from interactions between the protein and the confining wall, but rather arises from interactions between the confined solvent and the confined protein.

Table 1. Values for shifts in free energy of folding ($\Delta\Delta G_F$), transition state (Δx_{TS}), and barrier width ($\Delta\sigma$) derived from the P_{fold} correlations in Fig. 2

Measure	Bulk–protein confined	Bulk–protein and solvent confined	Protein confined–protein and solvent confined
$\Delta\Delta G_F$ (k_BT)	−1.01 ± 0.19	1.05 ± 0.47	2.11 ± 0.36
Δx_{TS}	−4.64 ± 1.40	0.68 ± 0.40	1.49 ± 1.10
$\Delta\sigma$	3.60 ± 0.73	1.04 ± 0.34	1.00 ± 0.53

$\Delta\Delta G_F$ values were calculated from the method by Berezhkovskii and Szabo (38), and barrier widths and transition state shifts were calculated from the method by Rhee and Pande (13). The error in $\Delta\Delta G_F$ is computed from a bootstrap error analysis, and the error in the transition state shift and barrier width is the rmsd from the fit.

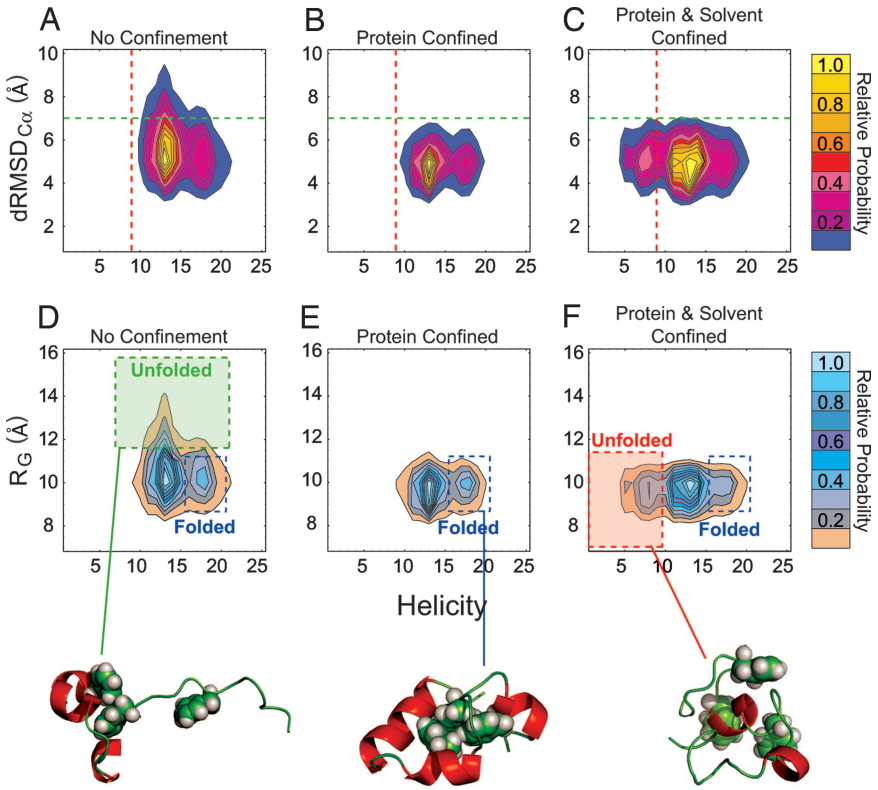

Fig. 3. The 2D distribution of states over all trajectories is shown for dRMSD$_{C\alpha}$ versus helicity and radius of gyration versus helicity. Because the trajectories are not at equilibrium, the contours do not imply differences in free energy. We have normalized the probability of finding a conformation from zero to one. Each contour represents one-10th of the maximum probability. (*A–C*) The dashed lines show the cutoffs used to define the unfolded state. The green line separates all states with a dRMSD$_{C\alpha} \geq$ 7 Å, and the red dashed line separates all states with less than nine helical residues. (*D–F*) The region bounded by the dashed blue box is the folded state. The region bounded by the dashed green box (*D*) is the expanded unfolded state found in simulations lacking confinement. The region bounded by the dashed red box is the compact unfolded state (*F*) found in simulations with both protein and solvent confined. Representative structures from each of these regions are shown with the residues comprising the hydrophobic core of the native state rendered as spheres and secondary structure calculated by DSSP.

For our system, the solvent-mediated effect is larger in magnitude than that of polymeric confinement. This effect is believed to arise as a result of the free-energy landscape created by confined water. Because the repulsive confining potential is effectively hydrophobic, water at the surface cannot have a full complement of hydrogen bonds. The protein is effectively pushed to this region, where there is a minimal free-energy penalty for disturbing the water's hydrogen-bond network. As the confining potential is purely repulsive, this effect must be occurring because of water–protein interactions rather than interactions between the protein and the confining wall. In previous works involving simple implicit models of solvent (23, 24), the net attraction between the protein and the wall must be included by hand. Our work using explicit solvent sheds light on the nature of this interaction and shows that for hydrophobic surfaces there can be an induced effective attraction, because of the nature of confined water. However, this may not be the case for all systems. Ideally, one would investigate how changing the hydrophobicity of the confining surface mediates this effect. Also, as chaperonins are water-permeable (25) it would be advantageous to perform these simulations at constant chemical potential for water (this would eliminate any pressure volume effects that cannot be treated with the current methodology). These modifications, however, involve a substantial increase in the complexity of our model and therefore must be treated in future work. Still, these results provide an interesting complement to the existing work that has focused on purely polymeric confinement and suggest that the solvent may not be merely a passive component for folding in chaperonins, but rather may play an important role in mechanism by which chaperonins aid protein folding.

Currently, a precise mechanism by which chaperonins help their substrates to fold is unknown, but several possible mechanisms have been proposed (26–28). Also, considering the fact that chaperonins act on many different substrates of various sizes (27, 29) it is feasible that more than one mechanism may be needed to describe chaperonin activity. Chaperonins are believed to rescue kinetically trapped non-native peptides by unfolding them. It has been proposed that chaperonins may do this entropically by binding nonnative peptide (30) or mechanically by exerting force on bound peptide during the chaperonin's own conformational changes (31). The results from our simulations indicate a third possibility. Confined solvent may create an energy landscape that is conducive to unfolding. If for some substrates chaperonins cause unfolding to a different unfolded state, this unfolded state may not be kinetically trapped nor aggregation prone. This idea is qualitatively consistent with both the fact that many iterations of chaperonin activity are frequently needed to fold substrates (26, 28), and bulk FRET experiments show that substrate is compacted (but not necessarily native-like) inside the cavity (30).

One may argue that the hydrophobic surface used in these simulations may not be relevant for modeling the behavior of proteins inside the closed chaperonin cavity (which is mostly hydrophilic). For this it is important to note that the prokaryotic chaperonin GroEL has long hydrophobic tails at its C terminus that are not resolved in the crystal structure (32). This hydrophobic surface may interact with solvent in such a way as to affect

folding in a way similar to that described above. It is also conceivable that upon confinement larger substrates (where the volume of the chaperonin cavity is only slightly larger than that of the native protein) may be more affected by polymer entropy effects, whereas smaller substrates may be more sensitive to solvent-mediated effects. Even if the solvent effect described herein is not the driving force in chaperonin mechanism, solvent effects may still alter the energy landscape seen by the confined protein and most likely also affect the overall mechanism.

Methods

We would like to compare the folding kinetics of our confined and unconfined systems. One approach is to project the simulation data to one or a few reaction coordinates. However, choosing a proper 1D reaction coordinate for high-dimensional protein systems has long been a challenge in theoretical chemistry (33). Here, we use P_{fold} calculation to circumvent the choice of reaction coordinate. P_{fold} is defined as the probability of folding before unfolding for a given protein conformation (34). A structure with a P_{fold} of 1 is folded (committed to the folded ensemble). Likewise a structure with a P_{fold} of 0 is unfolded (committed to the unfolded ensemble), and structure with a P_{fold} of 0.5 is a transition-state structure (equally likely to commit to the folded or unfolded state). In this method, we choose a definition of the folded and unfolded states rather than choosing a single structural metric to use as a reaction coordinate. For our system we used the following definitions for the folded and unfolded states (see *SI Text* for justification of these definitions):

$$\text{folded} \equiv (\text{RMSD}_{C\alpha(9-32)} \leq 3.0\text{Å}) \cap (\text{dRMSD}_{C\alpha} \leq 4.0\ \text{Å}) \cap (N_{\text{helices}} = 3)$$

$$\text{unfolded} \equiv (\text{dRMSD}_{C\alpha} \geq 7.0\text{Å}) \cup (\text{helicity} \leq 9).$$

Here $\text{RMSD}_{c\alpha(9-32)}$ is the coordinate rmsd of the α carbons of residues 9–32 from their positions in the native structure [the N- and C-terminal residues of the villin headpiece are less structured so this metric is limited to the central residues (35)]. N_{helices} is the number of stretches of consecutive α-helical residues as determined by DSSP, and helicity is the number of helical residues as determined by DSSP (36).

We selected structures from previous simulations of the villin headpiece (without confinement) with a full range of P_{fold} values (0 to 1). For each of these structures we performed a large number of concurrent simulations by using the Folding@Home distributing computing network (37). From these simulations we simply counted the number of trajectories that committed to the folded or unfolded state (according to our definition). We then calculated the probability of folding before unfolding (P_{fold}) for each structure by calculating the fractions of simulations that committed to either state.

For our set of starting structures, we have calculated the P_{fold} for each under bulk-like conditions (no confinement; Fig. 1*A*), protein-only confinement (Fig. 1*B*), and protein and solvent confinement (Fig. 1*C*). We examined the correlation between P_{fold} under these different confinement regimes. From these correlations we can infer how confinement affects the kinetics (mechanism) and thermodynamics of folding. We estimated changes in mechanism [in terms of shifts in barrier width ($\Delta\sigma$) and position (Δx_{TS})] and changes in thermodynamics ($\Delta\Delta G_{\text{F}}$) as a result of confinement. Changes in barrier width and position were calculated by using the technique described in ref. 13. $\Delta\Delta G_{\text{F}}$ was calculated by fitting the following relation from Berezhkovskii and Szabo (38) (see ref. 38 and *SI Text* for a derivation):

$$P'_{\text{fold}} = \frac{P_{\text{fold}}}{P_{\text{fold}} + e^{\beta\Delta\Delta G_{\text{F}}}(1 - P_{\text{fold}})}.$$

Here P'_{fold} is the perturbed value (i.e., protein-only confined, protein and solvent confined), and P_{fold} is the original value (no confinement).

These estimates of kinetics and thermodynamics rely on the approximation that perturbations to the transition state are small. Although this is often the case for point mutations (in the case of ϕ-value analysis) this assumption may not be as valid in the case of confinement. For this reason, these values are meant as qualitative measure of kinetic and thermodynamic changes resulting from confinement.

For more detailed materials and methods on the nature of the simulation methodology, as well as analysis techniques, see *SI Text* and SI Figs. 4–8.

We thank Prof. Ken Dill, Relly Brandman, Jeremy England, and Chris Snow for advice in preparing this manuscript, Holly Duddy for assistance with figure preparation, and the Folding@Home participants for contribution of central processing unit time. This work was supported by National Institutes of Health Roadmap on Nanomedicine Grant EF-0623664.

1. Fersht AR, Daggett V (2002) *Cell* 108:573–582.
2. Snow CD, Sorin EJ, Rhee YM, Pande VS (2005) *Annu Rev Biophys Biomol Struct* 34:43–69.
3. Zhou HX, Dill KA (2001) *Biochemistry* 40:11289–11293.
4. Klimov DK, Newfield D, Thirumalai D (2002) *Proc Natl Acad Sci USA* 99:8019–8024.
5. Baumketner A, Jewett A, Shea JE (2003) *J Mol Biol* 332:701–713.
6. Takagi F, Koga N, Takada S (2003) *Proc Natl Acad Sci USA* 100:11367–11372.
7. Thirumalai D, Klimov DK, Lorimer GH (2003) *Proc Natl Acad Sci USA* 100:11195–11197.
8. Ping G, Yuan JM, Sun Z, Wei Y (2004) *J Mol Recognit* 17:433–440.
9. Zhou HX (2004) *J Mol Recognit* 17:368–375.
10. Ziv G, Haran G, Thirumalai D (2005) *Proc Natl Acad Sci USA* 102:18956–18961.
11. Tang YC, Chang HC, Roeben A, Wischnewski D, Wischnewski N, Kerner MJ, Hartl FU, Hayer-Hartl M (2006) *Cell* 125:903–914.
12. Rhee YM, Sorin EJ, Jayachandran G, Lindahl E, Pande VS (2004) *Proc Natl Acad Sci USA* 101:6456–6461.
13. Rhee YM, Pande VS (2006) *J Chem Phys* 323:66–77.
14. Levinger NE (2002) *Science* 298:1722–1723.
15. Mashl RJ, Joseph S, Aluru NR, Jakobsson E (2003) *Nano Lett* 3:589–592.
16. Piletic IR, Tan HS, Fayer MD (2005) *J Phys Chem B Condens Matter Mater Surf Interfaces Biophys* 109:21273–21284.
17. Sorin EJ, Pande VS (2006) *J Am Chem Soc* 128:6316–6317.
18. McKnight CJ, Matsudaira PT, Kim PS (1997) *Nat Struct Biol* 4:180–184.
19. Jorgenson WL, Chandrasekhar J, Madura JD (1983) *J Chem Phys* 79:926–935.
20. Kubelka J, Eaton WA, Hofrichter J (2003) *J Mol Biol* 329:625–630.
21. Tang Y, Goger MJ, Raleigh DP (2006) *Biochemistry* 45:6940–6946.
22. Ptitsyn OB, Pain RH, Semisotnov GV, Zerovnik E, Razgulyaev OI (1990) *FEBS Lett* 262:20–24.
23. Cheung MS, Thirumalai D (2006) *J Mol Biol* 357:632–643.
24. Jewett AI, Baumketner A, Shea JE (2004) *Proc Natl Acad Sci USA* 101:13192–13197.
25. Horst R, Wider G, Fiaux J, Bertelsen EB, Horwich AL, Wuthrich K (2006) *Proc Natl Acad Sci USA* 103:15445–15450.
26. Hartl FU, Hayer-Hartl M (2002) *Science* 295:1852–1858.
27. Spiess C, Meyer AS, Reissmann S, Frydman J (2004) *Trends Cell Biol* 14:598–604.
28. Fenton WA, Horwich AL (2003) *Q Rev Biophys* 36:229–256.
29. Kerner MJ, Naylor DJ, Ishihama Y, Maier T, Chang HC, Stines AP, Georgopoulos C, Frishman D, Hayer-Hartl M, Mann M, Hartl FU (2005) *Cell* 122:209–220.
30. Lin Z, Rye HS (2004) *Mol Cell* 16:23–34.
31. Shtilerman M, Lorimer GH, Englander SW (1999) *Science* 284:822–825.
32. McLennan NF, Girshovich AS, Lissin NM, Charters Y, Masters M (1993) *Mol Microbiol* 7:49–58.
33. Bolhuis PG, Chandler D, Dellago C, Geissler PL (2002) *Annu Rev Phys Chem* 53:291–318.
34. Du R, Pande VS, Grosberg AY, Shakhnovich ES (1998) *J Chem Phys* 108:334–350.
35. Duan Y, Kollman PA (1998) *Science* 282:740–744.
36. Kabsch W, Sander C (1983) *Biopolymers* 22:2577–2637.
37. Shirts MR, Pande VS (2000) *Science* 290:1903–1904.
38. Berezhkovskii A, Szabo A (2006) *J Chem Phys* 125:104902.